Impact of Sumatra earthquake on CMB topography and core ellipticity

V. Cannelli, D. Melini, A. Piersanti

Convegno interno INGV
Geodinamica e struttura dell'interno della Terra
15 – 16 novembre 2006

Aim of the work

Characterization of the global impact of 2004 Sumatra earthquake event through the investigation of its effects on core-mantle boundary (**CMB**) shape and on the elliptical part of the gravity field ($\mathbf{J_2}$)

Introduction

2004 Sumatra earthquake (M_w = 9.3)

Measurable effects on many geophysical observables

i.e.

- Earth's free oscillations T>1000 s (*Park et al. 2005*)
- Jump in rotational pole secular motion (*Chao and Gross 2005*)
- Static offsets ~ 1mm GPS stations up to 5000 km away from epc. (*Banerjee at al. 2005; Boschi et al. 2006*)

Earth's interior?

Introduction

CMB topography → elastic limit (t = 0)

CMB topography → fluid limit (t → ∞)

Modeling approach

Semi-analytical theoretical model (*Piersanti et al. 1995; Boschi et al. 2000*)

Laplace-trasformed variables

perturbing body force

Equilibrium/perturbed values

Quasi-static deformations

Incompressibility

Self-gravitation

Viscoelastic constitutive eqn.

$$\rho_0 \tilde{\mathbf{f}} = -\rho_0 \nabla \tilde{\phi}_1 - \nabla\left(\tilde{\mathbf{u}} \cdot \rho_0 g_0 \mathbf{e}_r\right) + \nabla \cdot \tilde{\mathbf{T}}$$

$$\nabla \cdot \tilde{\mathbf{u}} = 0$$

$$\nabla^2 \tilde{\phi}_1 = 0$$

$$\tilde{\mathbf{T}} = 2\tilde{\mu}\tilde{\mathbf{E}} + \tilde{p}_1 \mathbf{I}$$

reference gravity acc.

deformation field

perturbation to grav. field

incremental stress field

strain tensor

incremental pressure

Boundary condition
(*continuity matrix*)
Earth surface ⇒ CMB surface

Stratification model

43 homogeneous layers and a uniform fluid core (μ_c=0 - ρ_c=10.93 kg/m^3)

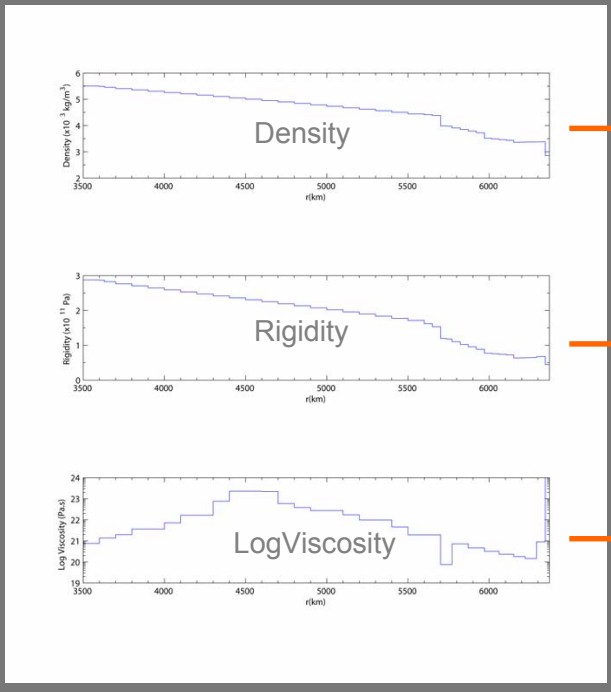

PREM (Preliminary Reference EarthModel, *Dziewonski & Anderson 1981*)

Viscosity model, *Mitrovica & Forte 2004* (joint inversion of convection and postglacial rebound data)

Seismic source

Five point sources (*Tsai et al. 2005*) fitting with the CMT method the long-period seismograms from the IRIS Global Seismographic Network

Table 2. Source Parameters for the Final, Five-Source Model[a]

Source	Strike	Dip	Rake	Moment	M_W	e
I	318	6.4	94	0.318	8.94	0.00
II	345	6.3	109	0.387	9.00	0.00
III	343	5.8	95	0.275	8.90	0.02
IV	15	8.4	132	0.105	8.62	0.04
V	35	8.1	155	0.081	8.54	0.01
Comp	343	6.1	107	1.15	9.31	0.02

[a]Strike, dip and rake are given in degrees. Moment is given in units of 10^{30} dyne-cm. e describes the relative size of the non-double-couple component of the moment tensor and is calculated as $\epsilon_2/\max(|\epsilon_1|,|\epsilon_3|)$ where ϵ are the ordered eigenvectors of the moment tensor. Values for a composite ("Comp") solution obtained by summing the moment-tensor components of the individual sources are also listed. The centroid location and time for the composite source are 8°N, 93.0°E and 214 s.

$M_w = 9.3$

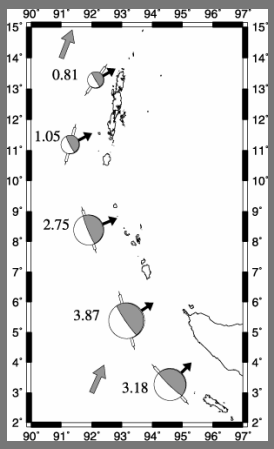

Perturbation of the CMB

Coseismic displacements

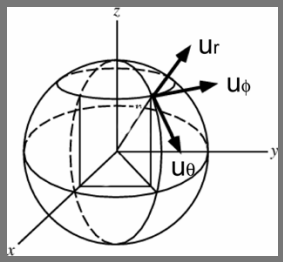

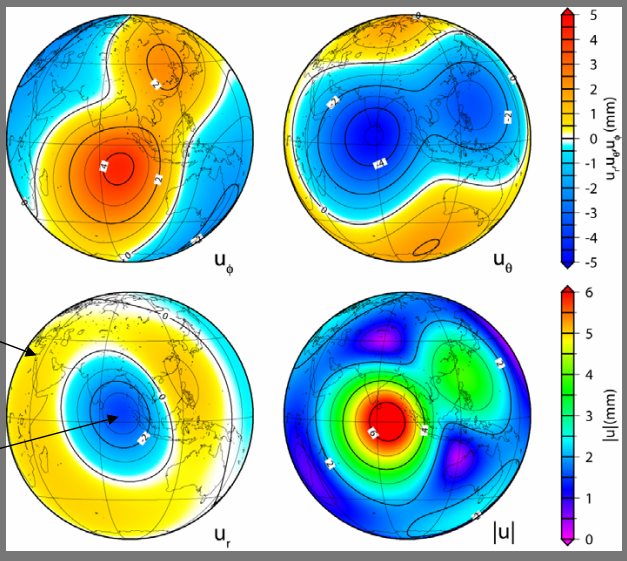

~ 0.5 mm

~ -4 mm

Perturbation of the CMB

Coseismic displacements

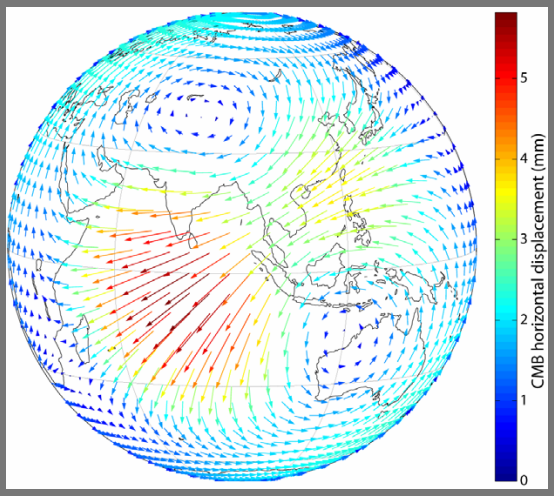

whole CMB surface affected by appreciable displacements
(fraction of mm far from source)

Symmetric properties

possible connection between CMB deformations and core flow perturbations? (*Dumberry & Bloxham 2004*)

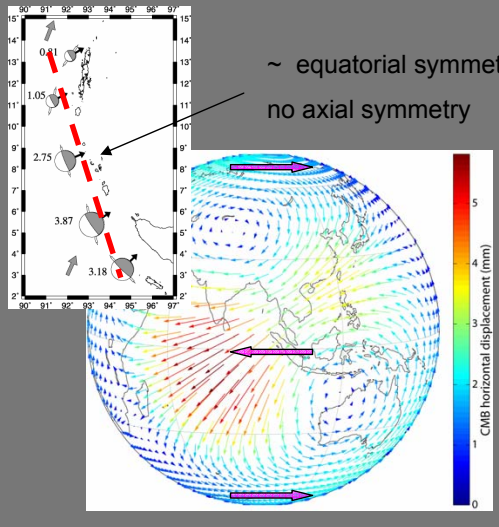

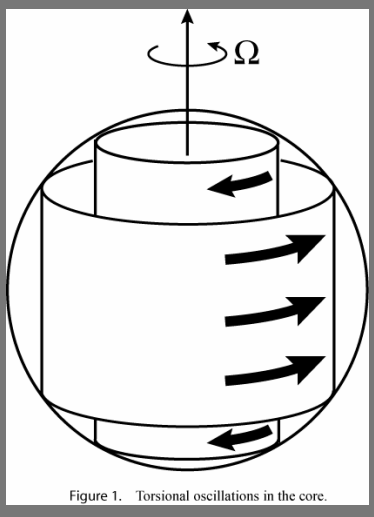

Figure 1. Torsional oscillations in the core.

Spectral harmonic decomposition

$$u(\theta,\phi) = \sum_{l=0}^{\infty} \sum_{m=-l}^{l} c_{lm} Y_{lm}(\theta,\phi)$$

$C_{lm} = (c^{r}_{lm}, c^{\theta}_{lm}, c^{\Phi}_{lm})$ harmonic coefficients

$$Y_{lm}(\theta,\phi) = \sqrt{\frac{2l+1}{4\pi}\frac{(l-m)!}{(l+m)!}} e^{im\phi} P_{lm}(\cos\theta)$$

P_{lm} = associated Legendre functions

Axial + equatorial symmetry $\overset{\text{def.}}{\Longleftrightarrow}$ even l, m=0

$$u_S(\theta) = \sum_{l\ \text{even}} c_{l0} Y_{l0}(\theta)$$

symmetric component

$$c_{l0} = \int u(\theta,\phi) Y_{l0}(\theta)\, d\Omega$$

C_{l0} = harmonic coefficients

Spectral harmonic decomposition

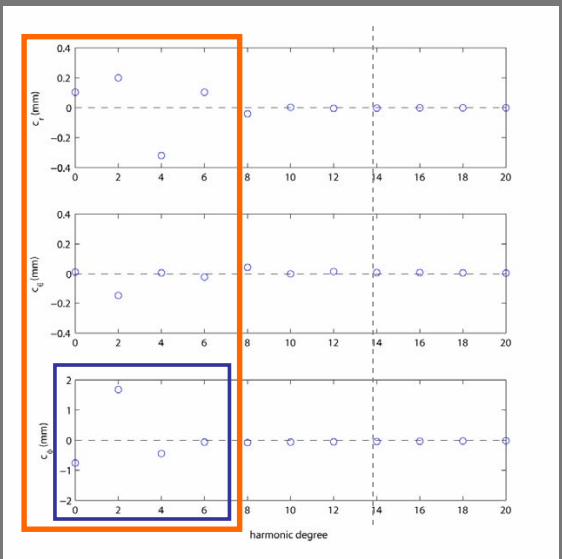

not negligible amount of deformation associated with the **lowest degrees** satisfies the **symmetry requirements**

main contribution from $\mathbf{u_\Phi}$ **component**

Spectral harmonic decomposition

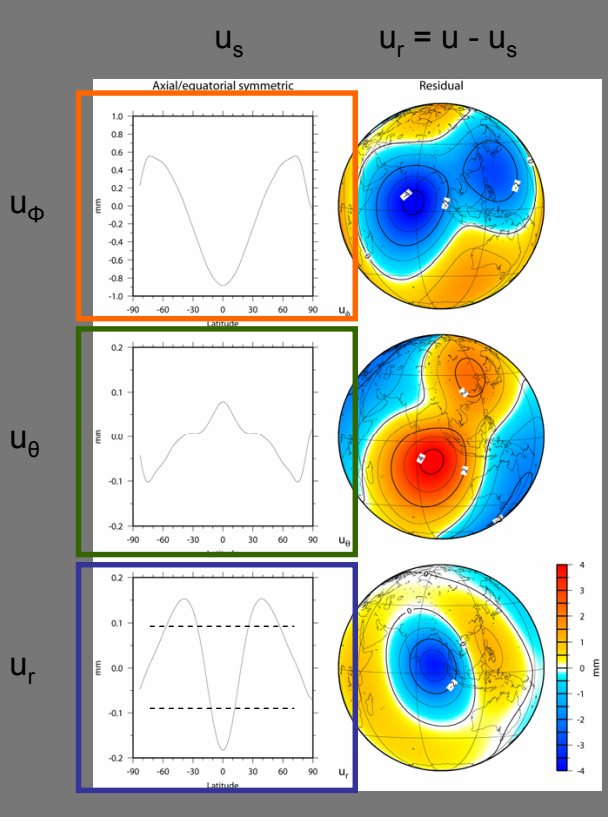

Spectral components satisfy **axial** and **equatorial symmetry** accounting for a considerable part of the total deformation

u_Φ peak ~ 0.8 mm in the equatorial zone

u_θ the smallest symmetric term

$u_r^{tor.osc.}$ ~ 0.5 mm
(Dumberry & Bloxham 2004)

u_r non negligible symmetric component (> 0.1 mm)

Perturbation of the CMB

Coseismic **Posteismic**

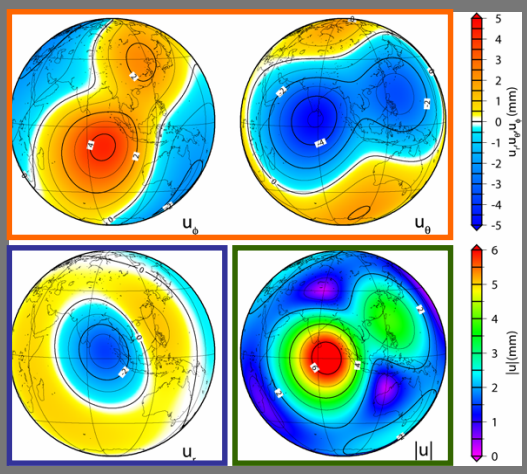

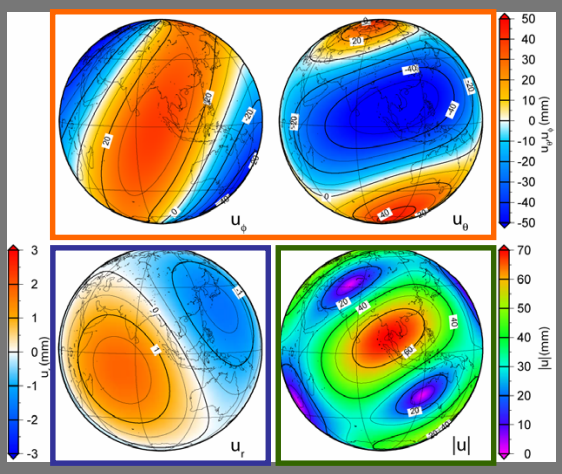

tangential components enhanced by the postseismic relaxation

radial component mean amplitude ~ the same of the elastic case

|u| ~ 10 greater than the elastic case (peak values ~ few centimeters)

Effects on J_2

main contribution to the deformation field comes from the **lowest degrees coefficients** of the spherical harmonic expansion

time-dependent evolution of the perturbation to the **elliptical part of the gravity field J_2**

2nd degree harmonic coefficient of the perturbation to φ_g

$$\Delta J_2 = \frac{R_T}{GM_T}\phi_{2,0}(R_T)$$

(Dumberry & Bloxham 2004)

axial (c) and equatorial (a) radius

$$e = \sqrt{1 - c^2/a^2} \qquad J_2 = e^2/5$$

e: Earth ellipticity

$\Delta J_2 > 0$ ←→ increasing **Earth oblateness**

incompressible model ➔ variation e_{Earth} ←→ variation e_{core}

Effects on J_2

long-term time-dependent evolution of the perturbation to J_2

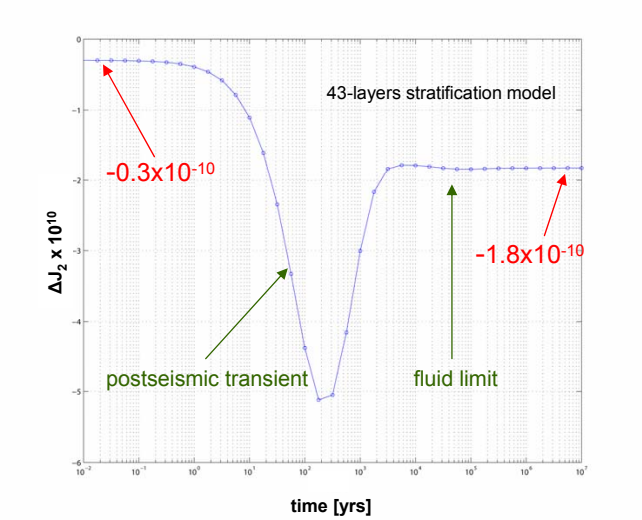

tendency of earthquakes to reduce the Earth's oblateness *(Chao & Gross 1987)*

$\Delta J^{el}_2 = -0.09 \times 10^{-10}$ *(Chao & Gross 2005)*

(resc. factor ~ 2.5 – M_w=9.0 → -0.23)

$\dot{J}_2 \sim -0.28 \times 10^{-10} yr^{-1}$ due to the secular linear drift *(Jeffreys 1970)*

$\dot{J}_2 \sim 0.25 \times 10^{-13} yr^{-1}$ mean annual J_2 variation for global seismic activity *(Alfonsi & Spada 1998)*

Effects on J_2

may viscoelastic relaxation leave a detectable signature on the J_2 measured time-histories?

short-timescale evolution of J_2 for **various asthenosphere viscosities**

elastic lithosphere (80 km)

viscoelastic asthenosphere (200 km, $\eta=10^{16},10^{17},10^{18}$ Pa s)

uniform mantle ($\eta = 10^{21}$ Pa s)

inviscid fluid core

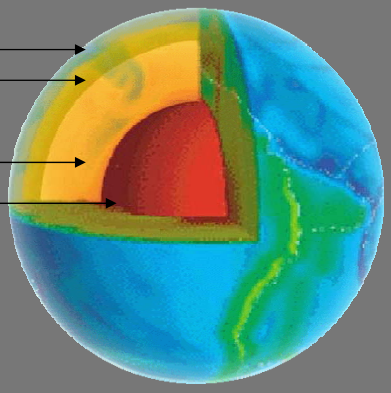

simplified three-layer stratification model

Effects on J_2

Time evolution of $\dot{J}_2$ variation

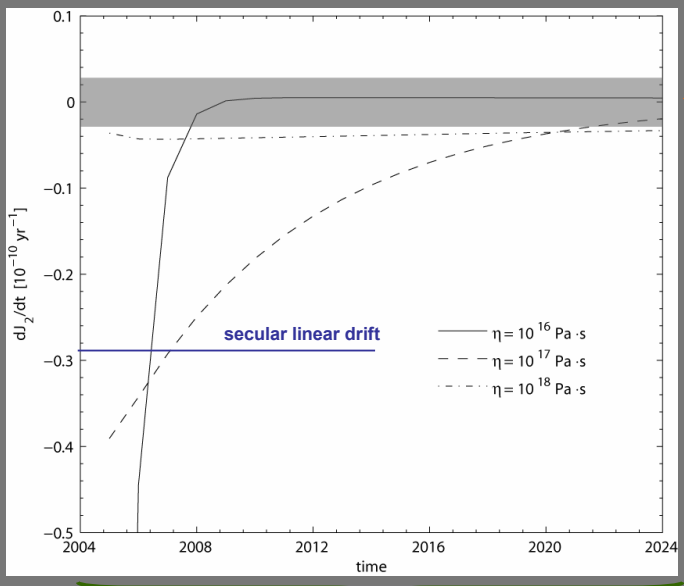

20 years

detectability threshold ± 0.03 x 10^{-10} yr^{-1} (10% measured value *Cheng et al. 1997*)

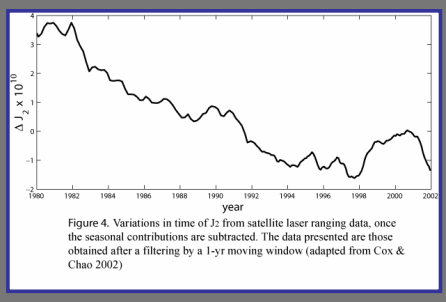

Figure 4. Variations in time of J2 from satellite laser ranging data, once the seasonal contributions are subtracted. The data presented are those obtained after a filtering by a 1-yr moving window (adapted from Cox & Chao 2002)

deviations of $\dot{J}_2$ available data from its secular drift ?

Effects on J_2

Table 1. Expected J_2 annual variation rate during 2005 and 2006 as a function of asthenosphere viscosity.

Asthenosphere viscosity (Pa s)	$\dot{J}_2$ 2005 ($10^{-10} \cdot yr^{-1}$)	$\dot{J}_2$ 2006 ($10^{-10} \cdot yr^{-1}$)
10^{15}	−2.679	+0.047
10^{16}	−2.160	−0.445
10^{17}	−0.391	−0.343
10^{18}	−0.036	−0.043
10^{19}	−0.005	−0.005
10^{20}	−0.003	−0.003
10^{21}	−0.002	−0.002
10^{22}	−0.002	−0.002

$\dot{J}_2^{sec.lin.drift} \sim -0.28 \times 10^{-10} yr^{-1}$

evident data signature is expected

just on the detectability threshold

should not produce a detectable signal

Conclusions

- CMB is globally affected by a significant amount of seismic deformation produced by the Sumatra earthquake
- most of this deformation is associated with large wavelength harmonics
- spectral components with axial and equatorial symmetry are of the same order of magnitude of that resulting from core torsional oscillations
- decrease of J_2 over time in agreement with reduction of Earth's oblateness by earthquakes
- time evolution of J_2 depends on the asthenospheric viscosity → from the analysis of measured $\dot{J}_2$ indication on constraints